Journal of Organometallic Chemistry, 481 (1994) 283–293

Steric effects in heteroboranes. Part 7 ☆

The synthesis and characterisation of arene–ruthenium complexes of C-substituted carbaboranes. Molecular structures of 1-Ph-3-(mes)-3,1,2-*closo*-$RuC_2B_9H_{10}$ (mes = C_6H_3-1,3,5) and 1-Ph-2-Me-3-(*p*-cym)-3,1,2-*closo*-$RuC_2B_9H_9$ (*p*-cym = C_6H_4Me-1-^iPr-4), the latter showing an incipient deformation

Jill Cowie, Bruce D. Reid, Jude M.S. Watmough, Alan J. Welch *

Department of Chemistry, University of Edinburgh, Edinburgh EH9 3JJ, UK

Received 15 March 1994

Abstract

The synthesis and characterization of Tl_2[7-Ph-7,8-*nido*-$C_2B_9H_{10}$], 3-(*p*-cym)-3,1,2-*closo*-$RuC_2B_9H_{11}$ (**1**), 1-Ph-3-(mes)-3,1,2-*closo*-$RuC_2B_9H_{10}$ (**2**), 1-Ph-3-(*p*-cym)-3,1,2-*closo*-$RuC_2B_9H_{10}$ (**3**) and 1-Ph-2-Me-3-(*p*-cym)-3,1,2-*closo*-$RuC_2B_9H_9$ (**4**) are reported. The ruthenium-containing species are obtained from the reactions between the appropriate [(arene)$RuCl_2]_2$ and either Tl_2[7,8-*nido*-$C_2B_9H_{11}$], Tl_2[7-Ph-7,8-*nido*-$C_2B_9H_{10}$] or Tl_2[7-Ph-8-Me-7,8-*nido*-$C_2B_9H_9$]. Crystallographic studies on **2** and **4** reveal that whereas the former contains an essentially undistorted {RuC_2B_9} framework, there is some indication that in the latter, a polyhedral deformation from *closo* towards *pseudocloso* has just begun. This idea gains support from comparison of the ^{11}B NMR shifts for **1**, **3** and **4** with those for reference carbaboranes.

Key words: Heteroboranes; Carbaboranes; Ruthenium; Arene complexes; Crystal structure

1. Introduction

Recently, we reported that unusual molecular structures and unusually facile polyhedral rearrangements can result from intramolecular crowding in carbametallaboranes. Specifically, the species 1,2-Ph_2-3-(C_5Me_5)-3,1,2-$RhC_2B_9H_9$ has been shown [2] to adopt a "*pseudocloso*" structure based on an icosahedron, but with an open Rh(3)C(1)B(6)C(2) face, and to show unusually high frequency shifts in its ^{11}B NMR spectrum, whereas 1-Ph-3,3-$(PMe_2Ph)_2$-3,1,2-$PtC_2B_9H_{10}$ undergoes isomerization [3] even at only 55°C to separate the cage carbon atoms.

These findings prompted us to make a systematic study of the effects on the spectroscopic and stereochemical properties and reactivity, gradually increasing the degree of crowding in a homologous series of carbametallaborane polyhedra, and we report below the synthesis and characterization of arene ruthenium species with phenyl- and methyl-phenyl-C_2B_9 ligands. Our initial targets were 3-(*p*-cym)-3,1,2-*closo*-$RuC_2B_9H_{11}$ (**1**), 1-Ph-3-(*p*-cym)-3,1,2-*closo*-$RuC_2B_9H_{10}$ (**3**) and 1-Ph-2-Me-3-(*p*-cym)-3,1,2-*closo*-$RuC_2B_9H_9$ (**4**). Structurally characterized analogues of **1** have previously been reported [4,5] and therefore it was not considered worthwhile to undertake a crystallographic study of this species. Compound **3** could only be obtained as very small crystals, so we also synthesized and structurally analysed 1-Ph-3-(mes)-3,1,2-*closo*-$RuC_2B_9H_{10}$ (**2**) as an alternative to **3**.

* Corresponding author. Present address: Department of Chemistry, Heriot-Watt University, Edinburgh EH14 4AS, UK.

☆ For Part 6, see Ref. [1].

0022-328X/94/$7.00
SSDI 0022-328X(94)24704-M

2. Experimental details

2.1. Synthesis and characterization

All reactions were carried out under dry, oxygen-free N_2 by use of standard Schlenk techniques, with some subsequent manipulations carried out in the open laboratory. Unless otherwise stated, all solvents were dried and distilled under N_2 just prior to use. NMR spectra were recorded on Bruker WP80SY or WH360 spectrometers as $CDCl_3$ solutions at 298 K, chemical are reported relative to external $SiMe_4$ (^1H) or $BF_3 \cdot OEt_2$ (^{11}B, ^{11}B-{^1H}). IR spectra were recorded as a KBr disk or as reference solutions in CH_2Cl_2 on a Perkin-Elmer 598 spectrophotometer. Microanalyses were performed by the departmental service. The starting materials Tl_2 [7,8-*nido*-$C_2B_9H_{11}$] [4], Tl_2 [7-Ph-8-Me-7,8-*nido*-$C_2B_9H_9$] [6], [(mes)$RuCl_2]_2$ [7] and [(*p*-cym)$RuCl_2]_2$ [8] were prepared by published methods or slight variants thereof.

2.1.1. Tl_2[7-Ph-7,8-nido-$C_2B_9H_{10}$]

A mixture of 1-Ph-1,2-*closo*-$C_2B_{10}H_{11}$ (1.76 g, 8.0 mmol) and KOH (2.69 g, 48 mmol) was stirred in EtOH (20 cm^3) for 0.5 h then heated under reflux for 15 h. The solution was allowed to cool, and EtOH was removed in vacuo to afford K_2[7-Ph-7,8-*nido*-$C_2B_9H_{10}$] as a waxy white solid, which was dissolved in H_2O (15 cm^3). The solution was filtered, and to the filtrate was added a solution of Tl[$OOCCH_3$] (4.21 g, 16 mmol) in H_2O (10 cm^3). The intensely bright yellow solid product, Tl_2[7-Ph-7,8-*nido*-$C_2B_9H_{10}$], which separated out was filtered off, washed successively with EtOH (3 × 15 cm^3) and Et_2O (3 × 15 cm^3), and dried in vacuo in a foil-covered container. Yield 4.0 g, 81%. Calculated for $C_8H_{15}B_9Tl_2$; 15.6% C, 2.45% H. Found; 15.0% C, 2.18% H. IR (KBr) ν_{max} at 2509, 2443, and 2381 (all B–H) cm^{-1}.

2.1.2. 3-(p-cym)-3,1,2-closo-$RuC_2B_9H_{11}$ (1)

To a mixture of [(*p*-cym)$RuCl_2]_2$ (0.29 g, 0.47 mmol) and Tl_2[7,8-*nido*-$C_2B_9H_{11}$] (0.50 g, 0.92 mmol) in a foil-covered Schlenk tube at −196°C was added CH_2Cl_2 (20 cm^3). The mixture was allowed to warm slowly to room temperature and stirred overnight. The solution was filtered and the orange filtrate concentrated to ca. 2 cm^3 in vacuo. Preparative thin layer chromatography (TLC) on silica, with CH_2Cl_2/n-hexane (60:40) as eluent, yielded a mobile yellow band with R_f ca. 0.8. This was collected and the recovered solid was purified by recrystallization (CH_2Cl_2/hexane at −30°C) to afford small yellow crystals of 3-(*p*-cym)-3,1,2-*closo*-$RuC_2B_9H_{11}$ (**1**). Yield 0.09 g, 28%. Calculated for $C_{12}H_{25}B_9Ru$; 39.0% C, 6.77% H. Found for **1**; 39.2% C, 6.85% H. I.r. (CH_2Cl_2) ν_{max} at 2530 (s, br) (B–H) cm^{-1}. NMR: ^1H; δ 5.93–5.88 (m, 4H, $MeC_6H_4CHMe_2$), 3.80 (br s, 2H, $C_{cage}H$), 2.85 (hept, 1H, $^3J_{HH} = 7$ Hz, $MeC_6H_4CHMe_2$), 2.32 (s, 3H, $MeC_6H_4CHMe_2$), 1.28 (d, $^3J_{HH} = 7$ Hz, 6H, $MeC_6H_4CHMe_2$) ppm. ^{11}B-{^1H}; δ 2.77 (1B), 1.25 (1B), −6.67 (2B), −8.24 (2B), −18.59 (2B), −23.21 (1B) ppm.

2.1.3. 1-Ph-3-(mes)-3,1,2-closo-$RuC_2B_9H_{10}$ (2)

To a mixture of [(mes)$RuCl_2]_2$ (0.88 g, 1.5 mmol) and Tl_2[7-Ph-7,8-*nido*-$C_2B_9H_{10}$] (1.85 g, 3.0 mmol) at −196°C in a foil-covered Schlenk tube was added CH_2Cl_2 (10 cm^3). The stirred mixture was allowed to warm to room temperature, resulting in a colour change and the appearance of a fine grey precipitate. After ca. 1 h, the mixture was filtered through Celite and the orange filtrate concentrated to ca. 2 cm^3 in vacuo. Preparative TLC (CH_2Cl_2/n-hexane, 60:40) revealed several bands, of which that with R_f 0.7 (pale brown) was collected and evaporated. The residue was recrystallized by solvent diffusion (CH_2Cl_2 solution | hexane, 1:4, −30°C) to yield 1-Ph-3-(mes)-3,1,2-*closo*-$RuC_2B_9H_{10}$ (**2**) as large, well-formed yellow crystals. Yield 0.37 g, 29%. Calculated for $C_{17}H_{27}B_9Ru$; 47.5% C, 6.33% H. Found for **2**; 47.1% C, 6.04% H. IR (CH_2Cl_2) ν_{max} at 2522 (s, br) (B–H) cm^{-1}. NMR: ^1H; δ 7.28–7.04 (m, 5H, C_6H_5), 5.23 (s, 3H, CH_3Me_3), 4.32 (br s, 1H, CH_{cage}), 2.04 (s, 9H, CH_3Me_3) ppm. ^{11}B-{^1H}; δ 3.19 (1B), 2.17 (1B), −4.25 (1B), −6.51 (1B), −8.35 (2B), −14.13 (1B), −18.70 (2B) ppm.

2.1.4. 1-Ph-3-(p-cym)-3,1,2-closo-$RuC_2B_9H_{10}$ (3)

In a procedure analogous to that used for **1**, a mixture of [(*p*-cym)$RuCl_2]_2$ (0.25 g, 0.40 mmol) and Tl_2[7-Ph-7,8-*nido*-$C_2B_9H_{10}$] (0.50 g, 0.81 mmol) in CH_2Cl_2 (20 cm^3) was allowed to warm from −196°C in a foil-covered Schlenk tube, and stirred overnight. The resulting peach coloured solution was filtered and concentrated to ca. 2 cm^3. Preparative TLC (CH_2Cl_2/n-hexane 60:40) yielded a complex mixture of bands, the most mobile of which ($R_f = 0.7$) yielded small yellow crystals of 1-Ph-3-(*p*-cym)-3,1,2-*closo*-$RuC_2B_9H_{10}$ (**3**) by slow diffusion of hexane into a CH_2Cl_2 solution (4:1) at −30°C. Yield 0.06 g, 18%. Calculated for $C_{18}H_{29}B_9Ru$; 48.7% C, 6.59% H. Found for **3**; 47.0% C, 6.92% H. IR (CH_2Cl_2) ν_{max} at 2970 (C–H) and 2545 (s, br) (B–H) cm^{-1}. NMR: ^1H; δ 7.27–7.10 (m, 5H, C_6H_5), 5.51–4.97 (m, 4H, $MeC_6H_4CHMe_2$), 4.44 (br s, 1H, $C_{cage}H$), 2.76 (m, 1H, $MeC_6H_4CHMe_2$), 2.35 (s, 3H, $MeC_6H_4CHMe_2$), 1.31 (app d, $^3J_{HH} = 7$ Hz, 6H, $MeC_6H_4CHMe_2$) ppm. ^{11}B-{^1H}; δ 2.71 (2B), −4.27 (1B), −6.91 (1B), −7.71 (1B), −8.15 (1B), −14.27 (1B), −18.24 (2B) ppm.

2.1.5. 1-Ph-2-Me-3-(p-cym)-3,1,2-closo-$RuC_2B_9H_9$ (4)

Similarly, a mixture of $[(p\text{-cym})RuCl_2]_2$ (0.29 g, 0.48 mmol) and Tl_2[7-Ph-8-Me-7,8-*nido*-$C_2B_9H_9$] (0.60 g, 0.95 mmol) in CH_2Cl_2 (20 cm^3) were allowed to warm from −196°C and stirred overnight at room temperature. The resulting deep red solution was filtered to remove the grey precipitate and the filtrate concentrated to ca. 2 cm^3 in vacuo. Preparative TLC (CH_2Cl_2/n-hexane 60:40) yielded two mobile bands. That at $R_f = 0.7$ was collected and yielded a solid, which was recrystallized from CH_2Cl_2/n-hexane (1:4) at −30°C to yield diffraction-quality yellow single crystals of 1-Ph-2-Me-3-(*p*-cym)-3,1,2-*closo*-$RuC_2B_9H_9$ (**4**).

Table 1
Crystallographic data and details of data collection and structure refinement

	2	3	4
Formula	$C_{17}H_{27}B_9Ru$	$C_{18}H_{29}B_9Ru$	$C_{19}H_{31}B_9Ru$
M	429.76	443.79	457.82
System	Orthorhombic	Monoclinic	Monoclinic
Space group	$P2_12_12_1$	$P2_1/c$	$P2_1$
a (Å)	9.300(4)	13.33(3)	14.803(6)
b (Å)	14.217(5)	9.439(3)	18.935(6)
c (Å)	15.194(3)	17.627(16)	7.944(3)
β (°)	90	108.21(13)	101.43(5)
V (Å^3)	2008.9	2107.7	2181.0
Z	4	4	4 (2 independent)
D_{calc} (g cm^{-3})	1.421	1.398	1.393
μ (Mo Kα) (cm^{-1})	7.64	7.30	7.07
F(000) (e)	872	904	936
$\theta_{orientation}$ (°)	14–15	6–11	9–22
T (K)	291 ± 1	291 ± 1	205 ± 1
$\theta_{data\ collection}$ (°)	1–25		1–25
h range	0 → +11		−17 → +17
k range	0 → +16		0 → +22
l range	0 → +18		0 → +9
ω scan speeds (° min^{-1})	0.92–2.35		0.78–2.35
Data measured	2044		4281
Data observed	2012		3412
Criterion for observed	$F > 2.0\sigma(F)$		$F > 2.0\sigma(F)$
Period (h)	47		97
U_H (Å^2)	0.082(6) (non-cage) 0.049(6) (cage)		0.0609(13)
g	0.001418		0.000960
R	0.0297		0.0419
R_w	0.0494		0.0484
S	0.977		1.070
Variables	278		279 (block 1), 280 (block 2)
Max. residue (e Å^{-3})	0.58		0.62 near Ru(3b)
Min. residue (e Å^{-3})	−0.60		−0.47

Table 2
Fractional coordinates of non-hydrogen atoms in compound **2**

	x	y	z
Ru(3)	0.57101(3)	0.46432(2)	−0.05340(2)
C(1)	0.6556(4)	0.5716(3)	−0.14189(24)
C(11)	0.5327(4)	0.6180(3)	−0.1890(3)
C(12)	0.4572(5)	0.6929(3)	−0.1499(3)
C(13)	0.3362(5)	0.7331(3)	−0.1919(3)
C(14)	0.2951(6)	0.7018(4)	−0.2710(3)
C(15)	0.3712(5)	0.6308(4)	−0.3144(3)
C(16)	0.4896(6)	0.5885(4)	−0.2729(3)
C(31)	0.4960(5)	0.3477(3)	0.0316(3)
C(32)	0.4519(5)	0.4340(3)	0.0682(3)
C(33)	0.3693(5)	0.5013(3)	0.0209(3)
C(34)	0.3314(5)	0.4793(4)	−0.0671(3)
C(35)	0.3724(4)	0.3928(3)	−0.1058(3)
C(36)	0.4563(5)	0.3282(3)	−0.0572(3)
C(311)	0.5844(6)	0.2802(3)	0.0838(4)
C(331)	0.3227(7)	0.5899(4)	0.0628(4)
C(351)	0.3299(6)	0.3707(4)	−0.2006(4)
C(2)	0.7069(5)	0.4638(3)	−0.1684(3)
B(12)	0.9430(6)	0.4788(5)	−0.0519(4)
B(11)	0.8918(6)	0.4581(4)	−0.1620(3)
B(4)	0.6918(5)	0.5955(3)	−0.0341(3)
B(6)	0.8079(5)	0.5601(4)	−0.2043(3)
B(5)	0.7990(6)	0.6435(3)	−0.1193(3)
B(7)	0.7873(5)	0.4096(3)	−0.0773(3)
B(9)	0.8817(6)	0.5935(4)	−0.0240(3)
B(10)	0.9526(6)	0.5739(4)	−0.1292(4)
B(8)	0.7820(5)	0.4945(4)	0.0108(3)

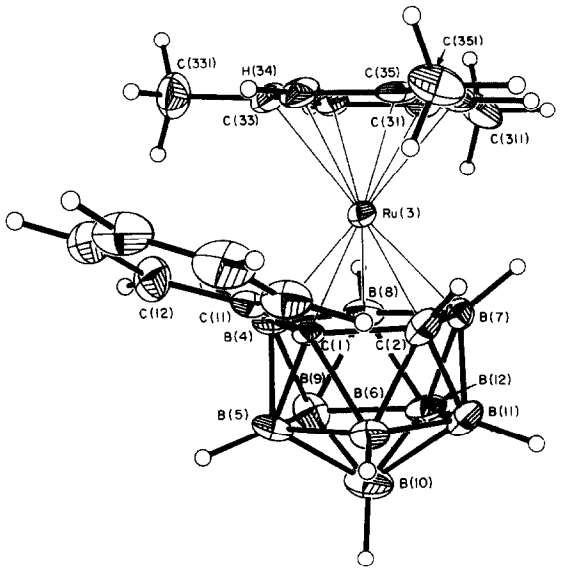

Fig. 1. Perspective view of the molecular structure of **2** (50% thermal ellipsoids) with sufficient atoms labelling to completely identify all atoms. Aromatic rings are labelled cyclically C(xy) (y = 1–6).

Table 3
Fractional coordinates of non-hydrogen atoms in compound **4**

	x	y	z
C(1a)	0.0932(5)	0.0889(4)	0.1179(9)
C(2a)	0.1741(6)	0.0743(5)	0.3083(9)
Ru(3a)	0.06136(4)	0.00000	0.26946(7)
B(4a)	0.0795(5)	0.0118(4)	0.0014(8)
B(5a)	0.1467(5)	0.0823(5)	−0.0446(9)
B(6a)	0.2036(6)	0.1224(5)	0.1448(9)
B(7a)	0.2125(6)	−0.0111(5)	0.3136(9)
B(8a)	0.1551(6)	−0.0514(5)	0.1215(9)
B(9a)	0.1889(6)	−0.0057(5)	−0.0455(9)
B(10a)	0.2683(6)	0.0622(6)	0.0369(9)
B(11a)	0.2778(6)	0.0579(6)	0.2596(9)
B(12a)	0.2690(6)	−0.0196(5)	0.1433(10)
C(12a)	0.0360(3)	0.2101(3)	0.1901(6)
C(13a)	−0.0335(3)	0.2610(3)	0.1675(6)
C(14a)	−0.1184(3)	0.2472(3)	0.0603(6)
C(15a)	−0.1339(3)	0.1825(3)	−0.0243(6)
C(16a)	−0.0644(3)	0.1315(3)	−0.0017(6)
C(11a)	0.0205(3)	0.1453(3)	0.1054(6)
C(21a)	0.1737(6)	0.1177(5)	0.4746(8)
C(31a)	−0.0547(5)	0.0357(4)	0.4078(8)
C(32a)	0.0130(5)	−0.0009(4)	0.5194(8)
C(33a)	0.0427(6)	−0.0706(4)	0.4844(9)
C(34a)	0.0009(5)	−0.1018(4)	0.3289(9)
C(35a)	−0.0639(4)	−0.0652(4)	0.2099(8)
C(36a)	−0.0921(5)	0.0031(4)	0.2510(8)
C(37a)	−0.0910(6)	0.1055(5)	0.4442(10)
C(40a)	0.0242(6)	−0.1787(4)	0.2910(10)
C(41a)	0.1128(7)	−0.2046(5)	0.4023(10)
C(44a)	−0.0552(7)	−0.2262(5)	0.3005(10)
C(1b)	0.4055(5)	0.3704(5)	0.4026(8)
C(2b)	0.3359(5)	0.3646(4)	0.2049(9)
Ru(3b)	0.43561(4)	0.45002(3)	0.22747(8)
B(4b)	0.4029(5)	0.4578(4)	0.4797(8)
B(5b)	0.3359(6)	0.3842(5)	0.5536(9)
B(6b)	0.2970(6)	0.3316(6)	0.3889(10)
B(7b)	0.2858(5)	0.4461(5)	0.1433(9)
B(8b)	0.3238(6)	0.5067(5)	0.3219(10)
B(9b)	0.2840(7)	0.4696(6)	0.5029(10)
B(10b)	0.2270(6)	0.3908(6)	0.4378(10)
B(11b)	0.2238(6)	0.3770(5)	0.2241(10)
B(12b)	0.2158(6)	0.4612(6)	0.2973(10)
C(12b)	0.4828(3)	0.24912(23)	0.4123(5)
C(13b)	0.5577(3)	0.20512(23)	0.4741(5)
C(14b)	0.6337(3)	0.23130(23)	0.5899(5)
C(15b)	0.6349(3)	0.30147(23)	0.6439(5)
C(16b)	0.5600(3)	0.34546(23)	0.5820(5)
C(11b)	0.4839(3)	0.31929(23)	0.4662(5)
C(21b)	0.3495(6)	0.3102(4)	0.0776(9)
C(31b)	0.5744(5)	0.4167(4)	0.1564(8)
C(32b)	0.5091(5)	0.4280(4)	0.0088(9)
C(33b)	0.4631(5)	0.4920(5)	−0.0171(8)
C(34b)	0.4790(5)	0.5494(5)	0.1068(9)
C(35b)	0.5385(5)	0.5333(4)	0.2501(9)
C(36b)	0.5884(5)	0.4703(5)	0.2826(9)
C(37b)	0.6328(6)	0.3503(5)	0.1847(10)
C(40b)	0.4323(6)	0.6181(5)	0.0722(10)
C(41b)	0.3479(7)	0.6186(6)	−0.0726(11)
C(44b)	0.5015(7)	0.6723(6)	0.0507(12)

Yield 0.06 g, 13%. Calculated for $C_{19}H_{31}B_9Ru$; 49.9% C, 6.83% H. Found for **4**; 49.4% C, 6.91% H. IR (CH_2Cl_2) ν_{max} at 2965 (C–H) and 2540 (s, br) (B–H) cm^{-1}. NMR: ^1H; δ 7.36–7.13 (m, 5H, C_6H_5), 5.76–5.23 (m, 4H, $MeC_6H_4CHMe_2$), 2.88 (m, 1H, MeC_6H_4-$CHMe_2$), 2.48 (s, 3H, $MeC_6H_4CHMe_2$), 1.64 (s, 3H, $C_{cage}Me$), 1.29–1.24 (m, 6H, $MeC_6H_4CHMe_2$) ppm. ^{11}B-{^1H}; δ 4.11 (2B), −2.05 (1B), −4.83 (1B), −6.50 (1B), −9.03 (1B), −11.30 (1B), −12.51 (1B), −16.07 (1B) ppm.

2.2. Crystallographic studies

All measurements were carried out at room temperature on an Enraf-Nonius CAD4 diffractometer

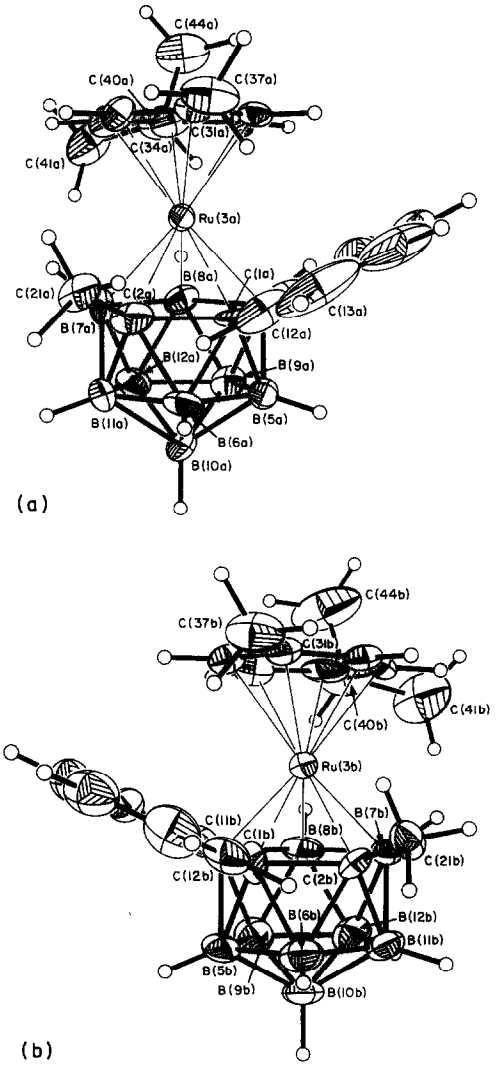

Fig. 2. Perspective views of single molecules of (a) **4a** and (b) **4b**, drawn with the same conventions as Fig. 1.

Table 4
Interatomic distances (Å) and selected interbond angles (°) in compound 2

Ru(3)–C(1)	2.181(4)	C(33)–C(34)	1.419(7)
Ru(3)–C(31)	2.215(4)	C(33)–C(331)	1.476(7)
Ru(3)–C(32)	2.196(4)	C(34)–C(35)	1.414(7)
Ru(3)–C(33)	2.251(5)	C(35)–C(36)	1.413(6)
Ru(3)–C(34)	2.248(5)	C(35)–C(351)	1.527(7)
Ru(3)–C(35)	2.253(4)	C(2)–B(11)	1.724(7)
Ru(3)–C(36)	2.210(4)	C(2)–B(6)	1.748(7)
Ru(3)–C(2)	2.157(5)	C(2)–B(7)	1.752(7)
Ru(3)–B(4)	2.196(5)	B(12)–B(11)	1.763(8)
Ru(3)–B(7)	2.188(5)	B(12)–B(7)	1.793(7)
Ru(3)–B(8)	2.232(5)	B(12)–B(9)	1.779(8)
C(1)–C(11)	1.501(5)	B(12)–B(10)	1.793(8)
C(1)–C(2)	1.656(6)	B(12)–B(8)	1.788(8)
C(1)–B(4)	1.706(6)	B(11)–B(6)	1.768(7)
C(1)–B(6)	1.713(6)	B(11)–B(7)	1.753(7)
C(1)–B(5)	1.714(6)	B(11)–B(10)	1.810(8)
C(11)–C(12)	1.407(6)	B(4)–B(5)	1.771(7)
C(11)–C(16)	1.402(7)	B(4)–B(9)	1.773(7)
C(12)–C(13)	1.414(7)	B(4)–B(8)	1.796(7)
C(13)–C(14)	1.338(7)	B(6)–B(5)	1.755(7)
C(14)–C(15)	1.398(7)	B(6)–B(10)	1.776(8)
C(15)–C(16)	1.404(7)	B(5)–B(9)	1.787(7)
C(31)–C(32)	1.408(6)	B(5)–B(10)	1.745(8)
C(31)–C(36)	1.427(6)	B(7)–B(8)	1.804(7)
C(31)–C(311)	1.491(7)	B(9)–B(10)	1.752(8)
C(32)–C(33)	1.421(6)	B(9)–B(8)	1.766(7)
C(1)–Ru(3)–C(2)	44.90(16)	B(11)–C(2)–B(7)	60.6(3)
C(1)–Ru(3)–B(4)	45.89(16)	B(11)–B(12)–B(7)	59.1(3)
C(31)–Ru(3)–C(32)	37.22(16)	B(11)–B(12)–B(10)	61.2(3)
C(31)–Ru(3)–C(36)	37.63(16)	B(7)–B(12)–B(8)	60.5(3)
C(32)–Ru(3)–C(33)	37.23(16)	B(9)–B(12)–B(10)	58.7(3)
C(33)–Ru(3)–C(34)	36.76(17)	B(9)–B(12)–B(8)	59.3(3)
C(34)–Ru(3)–C(35)	36.62(17)	C(2)–B(11)–B(6)	60.1(3)
C(35)–Ru(3)–C(36)	36.88(16)	C(2)–B(11)–B(7)	60.5(3)
C(2)–Ru(3)–B(7)	47.56(18)	B(12)–B(11)–B(7)	61.3(3)
B(4)–Ru(3)–B(8)	47.85(18)	B(12)–B(11)–B(10)	60.2(3)
B(7)–Ru(3)–B(8)	48.15(18)	B(6)–B(11)–B(10)	59.5(3)
Ru(3)–C(1)–C(11)	109.1(3)	Ru(3)–B(4)–C(1)	66.56(20)
Ru(3)–C(1)–C(2)	66.81(21)	Ru(3)–B(4)–B(8)	67.12(22)
Ru(3)–C(1)–B(4)	67.55(20)	C(1)–B(4)–B(5)	59.0(3)
C(11)–C(1)–C(2)	120.7(3)	B(5)–B(4)–B(9)	60.6(3)
C(11)–C(1)–B(4)	121.4(3)	B(9)–B(4)–B(8)	59.3(3)
C(11)–C(1)–B(6)	114.1(3)	C(1)–B(6)–C(2)	57.2(3)
C(11)–C(1)–B(5)	115.2(3)	C(1)–B(6)–B(5)	59.2(3)
C(2)–C(1)–B(6)	62.5(3)	C(2)–B(6)–B(11)	58.7(3)
B(4)–C(1)–B(5)	62.4(3)	B(11)–B(6)–B(10)	61.4(3)
B(6)–C(1)–B(5)	61.6(3)	B(5)–B(6)–B(10)	59.2(3)
C(1)–C(11)–C(12)	120.7(4)	C(1)–B(5)–B(4)	58.6(3)
C(1)–C(11)–C(16)	121.3(4)	C(1)–B(5)–B(6)	59.1(3)
C(12)–C(11)–C(16)	117.9(4)	B(4)–B(5)–B(9)	59.8(3)
C(11)–C(12)–C(13)	120.8(4)	B(6)–B(5)–B(10)	61.0(3)
C(12)–C(13)–C(14)	119.9(5)	B(9)–B(5)–B(10)	59.5(3)
C(13)–C(14)–C(15)	121.3(5)	Ru(3)–B(7)–C(2)	65.31(22)
C(14)–C(15)–C(16)	119.6(5)	Ru(3)–B(7)–B(8)	67.22(22)
C(11)–C(16)–C(15)	120.3(4)	C(2)–B(7)–b(11)	58.9(3)
Ru(3)–C(31)–C(311)	128.2(3)	B(12)–B(7)–B(11)	59.6(3)
C(32)–C(31)–C(36)	117.8(4)	B(12)–B(7)–B(8)	59.6(3)
C(32)–C(31)–C(311)	120.8(4)	B(12)–B(9)–B(10)	61.0(3)
C(36)–C(31)–C(311)	121.4(4)	B(12)–B(9)–B(8)	60.6(3)
C(31)–C(32)–C(33)	123.0(4)	B(4)–B(9)–B(5)	59.7(3)
Ru(3)–C(33)–C(331)	131.3(4)	B(4)–B(9)–B(8)	61.0(3)
C(32)–C(33)–C(34)	117.6(4)	B(5)–B(9)–B(10)	59.1(3)
C(32)–C(33)–C(331)	121.0(4)	B(12)–B(10)–B(11)	58.6(3)

Table 4 (continued)

C(34)–C(33)–C(331)	121.4(4)	B(12)–B(10)–B(9)	60.2(3)
C(33)–C(34)–C(35)	121.1(4)	B(11)–B(10)–B(6)	59.1(3)
Ru(3)–C(35)–C(351)	129.7(3)	B(6)–B(10)–B(5)	59.8(3)
C(34)–C(35)–C(36)	119.8(4)	B(5)–B(10)–B(9)	61.5(3)
C(34)–C(35)–C(351)	120.0(4)	Ru(3)–B(8)–B(4)	65.03(22)
C(36)–C(35)–C(351)	120.1(4)	Ru(3)–B(8)–B(7)	64.63(22)
C(31)–C(36)–C(35)	120.7(4)	B(12)–B(8)–B(7)	59.9(3)
Ru(3)–C(2)–C(1)	68.30(21)	B(12)–B(8)–B(9)	60.1(3)
Ru(3)–C(2)–B(7)	67.13(22)	B(4)–B(8)–B(9)	59.7(3)
C(1)–C(2)–B(6)	60.3(3)		
B(11)–C(2)–B(6)	61.2(3)		

equipped with graphite-monochromated Mo Kα X-radiation ($\lambda_{bar} = 0.71069$ Å) operating in the θ–2θ mode.

Table 1 lists details of the unit cell data for **2–4**, and, in the cases of compounds **2** and **4**, intensity data collection and structure refinement. In each case, the unit cell parameters and the orientation matrix for data collection were established by least-squares refinement of the setting angles of 25 strong, high angle, reflections. Remeasurement at intervals of the intensities of check reflections revealed no crystal decay in either case. Only data with $F \geq 2.0\sigma(F)$ were retained for structure solution and refinement.

Both crystal structures were solved by Patterson (metal atom) and difference Fourier (all other non-H atom) methods, and refined by full-matrix least-squares. Although the structure of **2** was solved and refined without any difficulty, that of **4** suffers from the effects of severe pseudosymmetry, since the arrangement of RuC_2B_9 icosahedra corresponds closely to $P2_1/n$. However, the true space group is only $P2_1$, with two crystallographically-independent molecules per asymmetric unit. This situation was greatly clarified by the use of DIRDIF [9]. An empirical absorption correction (DIFABS [10]) was applied to each data set following isotropic convergence. Phenyl rings were treated as rigid, planar hexagons (C–C 1.395 Å). Cage H atoms in **4** were located from difference Fourier maps and allowed positional refinement subject to a common B–H distance of 1.10(5) Å, whereas those in **2** were fixed in idealized positions 1.1 Å from their respective C or B atoms. All non-cage H atoms in both structures were fixed at idealized sites (C–H 1.08 Å). H atoms were assigned (variable) group thermal parameters (2 in **2**, 1 in **4**). All non-H atoms were refined with anisotropic thermal parameters, and in the final stages of refinement data were weighted such that $w^{-1} = [\sigma^2(F) + gF^2]$.

Atomic scattering factors for B, C, and H were those inlaid in SHELX-76 [11], whilst those for Ru were taked from *International Tables* [12]. Programs used in addition to those referenced above were CADABS [13], CALC [14], and SHELXTL [15]. Tables of final (non-H) atomic positional parameters appear as Tables 2 and 3. Tables of anisotropic thermal parameters and H atom positions, and full lists of interbond angles have been deposited at the Cambridge Crystallographic Data Centre.

3. Results and discussion

The anion [7-Ph-7,8-*nido*-$C_2B_9H_{10}]^{2-}$ is produced in high yield by decapitation of 1-Ph-1,2-*closo*-$C_2B_{10}H_{11}$ with 6 equivalents of KOH in refluxing EtOH. As previously shown to be the case for other C_2B_9 carbaborane dianions [2,4,16], [7-Ph-7,8-*nido*-$C_2B_9H_{10}]^{2-}$ is readily isolated as its thallium(I) salt, which is a convenient precursor for transition metal complexes of the $PhC_2B_9H_{10}$ ligand [3].

Thus, Tl_2[7,8-*nido*-$C_2B_9H_{11}$] and Tl_2[7-Ph-7,8-*nido*-$C_2B_9H_{10}$] react with the species [(arene)$RuCl_2]_2$ [arene = $C_6H_3Me_3$-1,3,5 (mes) or $C_6H_4Me^iPr$-1,4 (*p*-cym)] to afford the carbaruthenaborane compounds **1–3**, respectively, in moderate yield following purification involving preparative TLC and subsequent recrystallization. Similarly, Tl_2[7-Ph-8-Me-7,8-*nido*-$C_2B_9H_9$] [6] reacts with the *p*-cymene ruthenium dimer to afford the doubly C_{cage} substituted compound **4** in modest yield after similar work-up. The syntheses of **1–4** in this way parallel those of other 1-R-2-R′-3-(arene)-3,1,2-*closo*-$RuC_2B_9H_9$ compounds, specifically R = R′ = H, arene = C_6H_6 [4,17]; R = CH_2OCH_3, R′ = H, arene = *p*-cym [18]; and R = R′ = CH_2OCH_3, arene = *p*-cym [18]. A related method involves reaction between the same kind of metal substrate and the appropriate monoanionic carbaborane ligand in the presence of base, as exemplified by the synthesis [19] of 3-(C_6Me_6)-3,1,2-*closo*-$RuC_2B_9H_{11}$.

Compounds **1–4** were characterized by microanalysis, IR, ^{1}H NMR and ^{11}B/^{11}B-{^{1}H} NMR spectroscopies, as detailed in Section 2. In the ^{11}B spectra all

Table 5
Interatomic distances (Å) and selected interbond angles (°) in compound **4**

C(1a)–C(2a)	1.754(11)	C(1b)–C(2b)	1.702(10)
C(1a)–Ru(3a)	2.175(7)	C(1b)–Ru(3b)	2.157(8)
C(1a)–B(4a)	1.719(10)	C(1b)–B(4b)	1.769(11)
C(1a)–B(5a)	1.648(11)	C(1b)–B(5b)	1.750(12)
C(1a)–B(6a)	1.725(11)	C(1b)–B(6b)	1.748(12)
C(1a)–C(11a)	1.505(9)	C(1b)–C(11b)	1.517(9)
C(2a)–Ru(3a)	2.157(8)	C(2b)–Ru(3b)	2.172(7)
C(2a)–B(6a)	1.713(12)	C(2b)–B(6b)	1.786(12)
C(2a)–B(7a)	1.712(12)	C(2b)–B(7b)	1.740(11)
C(2a)–B(11a)	1.684(13)	C(2b)–B(11b)	1.711(12)
C(2a)–C(21a)	1.557(12)	C(2b)–C(21b)	1.485(11)
Ru(3a)–B(4a)	2.211(8)	Ru(3b)–B(4b)	2.159(8)
Ru(3a)–B(7a)	2.204(9)	Ru(3b)–B(7b)	2.185(8)
Ru(3a)–B(8a)	2.213(8)	Ru(3b)–B(8b)	2.224(9)
Ru(3a)–C(31a)	2.315(7)	Ru(3b)–C(31b)	2.322(7)
Ru(3a)–C(32a)	2.241(8)	Ru(3b)–C(32b)	2.264(7)
Ru(3a)–C(33a)	2.228(8)	Ru(3b)–C(33b)	2.211(8)
Ru(3a)–C(34a)	2.214(7)	Ru(3b)–C(34b)	2.261(8)
Ru(3a)–C(35a)	2.199(7)	Ru(3b)–C(35b)	2.174(7)
Ru(3a)–C(36a)	2.246(7)	Ru(3b)–C(36b)	2.248(8)
B(4a)–B(5a)	1.746(11)	B(4b)–B(5b)	1.870(12)
B(4a)–B(8a)	1.779(11)	B(4b)–B(8b)	1.793(12)
B(4a)–B(9a)	1.763(11)	B(4b)–B(9b)	1.817(12)
B(5a)–B(6a)	1.746(12)	B(5b)–B(6b)	1.655(13)
B(5a)–B(9a)	1.780(12)	B(5b)–B(9b)	1.799(13)
B(5a)–B(10a)	1.826(12)	B(5b)–B(10b)	1.694(13)
B(6a)–B(10a)	1.811(12)	B(6b)–B(10b)	1.625(13)
B(6a)–B(11a)	1.770(13)	B(6b)–B(11b)	1.750(13)
B(7a)–B(8a)	1.765(12)	B(7b)–B(8b)	1.826(12)
B(7a)–B(11a)	1.728(13)	B(7b)–B(11b)	1.788(12)
B(7a)–B(12a)	1.733(12)	B(7b)–B(12b)	1.776(12)
B(8a)–B(9a)	1.738(12)	B(8b)–B(9b)	1.802(13)
B(8a)–B(12a)	1.765(12)	B(8b)–B(12b)	1.791(13)
B(9a)–B(10a)	1.776(12)	B(9b)–B(10b)	1.740(13)
B(9a)–B(12a)	1.737(12)	B(9b)–B(12b)	1.749(14)
B(10a)–B(11a)	1.749(13)	B(10b)–B(11b)	1.709(13)
B(10a)–B(12a)	1.763(13)	B(10b)–B(12b)	1.725(13)
B(11a)–B(12a)	1.725(13)	B(11b)–B(12b)	1.709(13)
C(31a)–C(32a)	1.384(10)	C(31b)–C(32b)	1.380(10)
C(31a)–C(36a)	1.403(10)	C(31b)–C(36b)	1.413(11)
C(31a)–C(37a)	1.476(11)	C(31b)–C(37b)	1.517(12)
C(32a)–C(33a)	1.434(11)	C(32b)–C(33b)	1.384(11)
C(33a)–C(34a)	1.398(11)	C(33b)–C(34b)	1.453(11)
C(34a)–C(35a)	1.390(10)	C(34b)–C(35b)	1.330(11)
C(34a)–C(40a)	1.540(11)	C(34b)–C(40b)	1.473(12)
C(35a)–C(36a)	1.417(10)	C(35b)–C(36b)	1.398(11)
C(40a)–C(41a)	1.510(12)	C(40b)–C(41b)	1.521(14)
C(40a)–C(44a)	1.493(12)	C(40b)–C(44b)	1.481(14)
C(2a)–C(1a)–Ru(3a)	65.6(3)	C(2a)–B(11a)–B(6a)	59.4(5)
C(2a)–C(1a)–B(6a)	59.0(4)	C(2a)–B(11a)–B(7a)	60.2(5)
C(2a)–C(1a)–C(11a)	121.6(5)	B(6a)–B(11a)–B(10a)	61.9(5)
Ru(3a)–C(1a)–B(4a)	68.0(3)	B(7a)–B(11a)–B(12a)	60.3(5)
Ru(3a)–C(1a)–C(11a)	110.8(4)	B(10a)–B(11a)–B(12a)	61.0(5)
B(4a)–C(1a)–B(5a)	62.4(5)	B(7a)–B(12a)–B(8a)	60.6(5)
B(4a)–C(1a)–C(11a)	124.1(5)	B(7a)–B(12a)–B(11a)	59.9(5)
B(5a)–C(1a)–B(6a)	62.3(5)	B(8a)–B(12a)–B(9a)	59.5(5)
B(5a)–C(1a)–C(11a)	116.7(6)	B(9a)–B(12a)–B(10a)	61.0(5)
B(6a)–C(1a)–C(11a)	113.1(5)	B(10a)–B(12a)–B(11a)	60.2(5)
C(1a)–C(2a)–Ru(3a)	66.7(4)	C(1a)–C(11a)–C(12a)	123.1(5)
C(1a)–C(2a)–B(6a)	59.7(5)	C(1a)–C(11a)–C(16a)	116.9(5)
C(1a)–C(2a)–C(21a)	122.2(6)	Ru(3a)–C(31a)–C(37a)	133.4(5)
Ru(3a)–C(2a)–B(7a)	68.3(4)	C(32a)–C(31a)–C(36a)	117.1(7)
Ru(3a)–C(2a)–C(21a)	109.5(5)	C(32a)–C(31a)–C(37a)	124.6(7)

Table 5 (continued)

B(6a)–C(2a)–B(11a)	62.8(5)	C(36a)–C(31a)–C(37a)	118.2(7)
B(6a)–C(2a)–C(21a)	114.0(6)	C(31a)–C(32a)–C(33a)	123.2(7)
B(7a)–C(2a)–B(11a)	61.2(5)	C(32a)–C(33a)–C(34a)	117.4(7)
B(7a)–C(2a)–C(21a)	122.4(6)	Ru(3a)–C(34a)–C(40a)	131.7(5)
B(11a)–C(2a)–C(21a)	116.7(7)	C(33a)–C(34a)–C(35a)	121.0(7)
C(1a)–Ru(3a)–C(2a)	47.8(3)	C(33a)–C(34a)–C(40a)	119.7(7)
C(1a)–Ru(3a)–B(4a)	46.2(3)	C(35a)–C(34a)–C(40a)	119.2(7)
C(2a)–Ru(3a)–B(7a)	46.2(3)	C(34a)–C(35a)–C(36a)	119.5(6)
B(4a)–Ru(3a)–B(8a)	47.4(3)	C(31a)–C(36a)–C(35a)	121.6(7)
B(7a)–Ru(3a)–B(8a)	47.1(3)	C(34a)–C(40a)–C(41a)	113.3(7)
C(31a)–Ru(3a)–C(32a)	35.3(3)	C(34a)–C(40a)–C(44a)	110.5(7)
C(31a)–Ru(3a)–C(36a)	35.8(3)	C(41a)–C(40a)–C(44a)	112.0(7)
C(32a)–Ru(3a)–C(33a)	37.4(3)	C(2b)–C(1b)–Ru(3b)	67.3(4)
C(33a)–Ru(3a)–C(34a)	36.7(3)	C(2b)–C(1b)–B(6b)	62.3(5)
C(34a)–Ru(3a)–C(35a)	36.7(3)	C(2b)–C(1b)–C(11b)	123.3(6)
C(35a)–Ru(3a)–C(36a)	37.2(3)	Ru(3b)–C(1b)–B(4b)	65.9(4)
C(1a)–B(4a)–Ru(3a)	65.8(3)	Ru(3b)–C(1b)–C(11b)	114.8(4)
C(1a)–B(4a)–B(5a)	56.8(4)	B(4b)–C(1b)–B(5b)	64.2(5)
Ru(3a)–B(4a)–B(8a)	66.4(4)	B(4b)–C(1b)–C(11b)	123.3(6)
B(5a)–B(4a)–B(9a)	60.9(5)	B(5b)–C(1b)–B(6b)	56.5(5)
B(8a)–B(4a)–B(9a)	58.8(5)	B(5b)–C(1b)–C(11b)	112.4(6)
C(1a)–B(5a)–B(4a)	60.8(5)	B(6b)–C(1b)–C(11b)	112.6(6)
C(1a)–B(5a)–B(6a)	61.0(5)	C(1b)–C(2b)–Ru(3b)	66.4(4)
B(4a)–B(5a)–B(9a)	60.0(5)	C(1b)–C(2b)–B(6b)	60.1(5)
B(6a)–B(5a)–B(10a)	60.9(5)	C(1b)–C(2b)–C(21b)	122.3(6)
B(9a)–B(5a)–B(10a)	59.0(5)	Ru(3b)–C(2b)–B(7b)	66.9(4)
C(1a)–B(6a)–C(2a)	61.4(5)	Ru(3b)–C(2b)–C(21b)	113.0(5)
C(1a)–B(6a)–B(5a)	56.7(5)	B(6b)–C(2b)–B(11b)	60.0(5)
C(2a)–B(6a)–B(11a)	57.8(5)	B(6b)–C(2b)–C(21b)	115.1(6)
B(5a)–B(6a)–B(10a)	61.8(5)	B(7b)–C(2b)–B(11b)	62.4(5)
B(10a)–B(6a)–B(11a)	58.5(5)	B(7b)–C(2b)–C(21b)	122.1(6)
C(2a)–B(7a)–Ru(3a)	65.4(4)	B(11b)–C(2b)–C(21b)	114.9(6)
C(2a)–B(7a)–B(11a)	58.6(5)	C(1b)–Ru(3b)–C(2b)	46.3(3)
Ru(3a)–B(7a)–B(8a)	66.7(4)	C(1b)–Ru(3b)–B(4b)	48.4(3)
B(8a)–B(7a)–B(12a)	60.6(5)	C(2b)–Ru(3b)–B(7b)	47.1(3)
B(11a)–B(7a)–B(12a)	59.8(5)	B(4b)–Ru(3b)–B(8b)	48.3(3)
Ru(3a)–B(8a)–B(4a)	66.2(4)	B(7b)–Ru(3b)–B(8b)	48.9(3)
Ru(3a)–B(8a)–B(7a)	66.2(4)	C(31b)–Ru(3b)–C(32b)	35.0(3)
B(4a)–B(8a)–B(9a)	60.1(5)	C(31b)–Ru(3b)–C(36b)	36.0(3)
B(7a)–B(8a)–B(12a)	58.8(5)	C(32b)–Ru(3b)–C(33b)	36.0(3)
B(9a)–B(8a)–B(12a)	59.4(5)	C(33b)–Ru(3b)–C(34b)	37.9(3)
B(4a)–B(9a)–B(5a)	59.1(5)	C(34b)–Ru(3b)–C(35b)	34.8(3)
B(4a)–B(9a)–B(8a)	61.1(5)	C(35b)–Ru(3b)–C(36b)	36.8(3)
B(5a)–B(9a)–B(10a)	61.8(5)	C(1b)–B(4b)–Ru(3b)	65.8(4)
B(8a)–B(9a)–B(12a)	61.0(5)	C(1b)–B(4b)–B(5b)	57.4(4)
B(10a)–B(9a)–B(12a)	60.2(5)	Ru(3b)–B(4b)–B(8b)	67.8(4)
B(5a)–B(10a)–B(6a)	57.4(5)	B(5b)–B(4b)–B(9b)	58.4(5)
B(5a)–B(10a)–B(9a)	59.2(5)	B(8b)–B(4b)–B(9b)	59.9(5)
B(6a)–B(10a)–B(11a)	59.6(5)	C(1b)–B(5b)–B(4b)	58.4(4)
B(9a)–B(10a)–B(12a)	58.8(5)	C(1b)–B(5b)–B(6b)	61.7(5)
B(11a)–B(10a)–B(12a)	58.8(5)	B(4b)–B(5b)–B(9b)	59.3(5)
B(6b)–B(5b)–B(10b)	58.0(5)	B(7b)–B(11b)–B(12b)	61.0(5)
B(9b)–B(5b)–B(10b)	59.7(5)	B(10b)–B(11b)–B(12b)	60.6(5)
C(1b)–B(6b)–C(2b)	57.6(4)	B(7b)–B(12b)–B(8b)	61.6(5)
C(1b)–B(6b)–B(5b)	61.8(5)	B(7b)–B(12b)–B(11b)	61.7(5)
C(2b)–B(6b)–B(11b)	57.9(5)	B(8b)–B(12b)–B(9b)	61.2(5)
B(5b)–B(6b)–B(10b)	62.2(6)	B(9b)–B(12b)–B(10b)	60.1(5)
B(10b)–B(6b)–B(11b)	60.7(5)	B(10b)–B(12b)–B(11b)	59.7(5)
C(2b)–B(7b)–Ru(3b)	66.1(4)	C(13b)–C(12b)–C(11b)	120.0(4)
C(2b)–B(7b)–B(11b)	58.0(4)	C(12b)–C(13b)–C(14b)	120.0(4)
Ru(3b)–B(7b)–B(8b)	66.6(4)	C(13b)–C(14b)–C(15b)	120.0(4)
B(8b)–B(7b)–B(12b)	59.6(5)	C(14b)–C(15b)–C(16b)	120.0(4)
B(11b)–B(7b)–B(12b)	57.3(5)	C(15b)–C(16b)–C(11b)	120.0(4)
Ru(3b)–B(8b)–B(4b)	64.0(4)	C(1b)–C(11b)–C(12b)	122.9(4)
Ru(3b)–B(8b)–B(7b)	64.4(4)	C(1b)–C(11b)–C(16b)	117.1(4)
B(4b)–B(8b)–B(9b)	60.7(5)	C(12b)–C(11b)–C(16b)	120.0(4)

Table 5 (continued)

B(7b)–B(8b)–B(12b)	58.8(5)	Ru(3b)–C(31b)–C(37b)	133.9(5)
B(9b)–B(8b)–B(12b)	58.2(5)	C(32b)–C(31b)–C(36b)	118.1(7)
B(4b)–B(9b)–B(5b)	62.3(5)	C(32b)–C(31b)–C(37b)	122.4(7)
B(4b)–B(9b)–B(8b)	59.4(5)	C(36b)–C(31b)–C(37b)	119.5(7)
B(5b)–B(9b)–B(10b)	57.2(5)	C(31b)–C(32b)–C(33b)	120.1(7)
B(8b)–B(9b)–B(12b)	60.6(5)	C(32b)–C(33b)–C(34b)	123.0(7)
B(10b)–B(9b)–B(12b)	59.3(5)	Ru(3b)–C(34b)–C(40b)	130.7(6)
B(5b)–B(10b)–B(6b)	59.8(5)	C(33b)–C(34b)–C(35b)	113.5(7)
B(5b)–B(10b)–B(9b)	63.2(5)	C(33b)–C(34b)–C(40b)	121.8(7)
B(6b)–B(10b)–B(11b)	63.3(6)	C(35b)–C(34b)–C(40b)	124.6(7)
B(9b)–B(10b)–B(12b)	60.6(5)	C(34b)–C(35b)–C(36b)	126.1(7)
B(11b)–B(10b)–B(12b)	59.7(5)	C(31b)–C(36b)–C(35b)	118.9(7)
C(2b)–B(11b)–B(6b)	62.1(5)	C(34b)–C(40b)–C(41b)	115.5(8)
C(2b)–B(11b)–B(7b)	59.6(5)	C(34b)–C(40b)–C(44b)	108.9(8)
B(6b)–B(11b)–B(10b)	56.0(5)	C(41b)–C(40b)–C(44b)	113.0(8)

signals appear as doublets with the expected $^1J_{BH}$ coupling of 115–170 Hz. Compounds **2–4** were also subjected to crystallographic analysis (Table 1) but only **2** and **4** afforded single crystals of suitable size for the collection of intensity data.

Figs. 1 and 2 present similar perspective views of each compound (two crystallographically independent molecules in the case of **4**) and Tables 4 and 5 list interatomic distances and selected interbond angles.

The structure of compound **2** was determined primarily to reveal any stereochemical consequence of substitution of a single phenyl group at cage carbon in arene carbaruthenaboranes. We have previously reported [2] that in the diphenyl species 1,2-Ph_2-3-(C_5Me_5)-3,1,2-*pseudocloso*-$RhC_2B_9H_9$ there is a substantial polyhedral deformation and we have recently shown [20] that in related arene compounds 1,2-Ph_2-3-(arene)-3,1,2-*pseudocloso*-$RuC_2B_9H_9$, (arene = C_6H_6, *p*-cym and C_6Me_6) there is a similar deformation. Although we believe that these cluster deformations, in which the C(1)–C(2) distance is raised to ca. 2.5 Å and M(3)...B(6) is concomitantly reduced to ca. 2.9 Å, are a result principally of intramolecular steric crowding, it is necessary also to consider the possible electronic influence of C_{cage}-phenyl substitution, particularly as no other transition metal complexes of the diphenyl C_2B_9 ligand have been reported.

In compound **2** the geometry of the RuC_2B_9 core is essentially undistorted, and thus this molecular structure serves as a suitable reference with which to compare structures in which H(2) is replaced by bulkier groups. The C(1)–C(2) separation in **2** is 1.656(6) Å, identical with that [5] [1.657(10) Å] in 3-(C_6Me_6)-3,1,2-*closo*-$RuC_2B_9H_{11}$, very close to that [17] [1.644(16) Å] in 3-(mes)-3,1,2-*closo*-$FeC_2B_9H_{11}$ and that [21] [1.646(8) Å] in the parent carbaborane 1-Ph-1,2-*closo*-$C_2B_{10}H_{11}$, and only marginally longer than that [4] [1.626(4) Å] in 3-(C_6H_6)-3,1,2-*closo*-$RuC_2B_9H_{11}$. Ru(3)...B(6) is 3.459 Å. A root mean square misfit calculation [22] between the {C_2B_9} fragments of **2** and those of 3-(C_6H_6)-3,1,2-*closo*-$RuC_2B_9H_{11}$ and 3-(C_6Me_6)-3,1,2-*closo*-$RuC_2B_9H_{11}$ affords misfits of only 0.034 and 0.028 Å, respectively.

We describe the conformation of cage-bound phenyl rings in arylcarbaboranes and their derivatives in terms of θ, the modulus of the average C_{cage}–C_{cage}–C–C torsion angle [23]; thus, if $\theta = 90°$, the plane of the phenyl ring eclipses the C(1)–C(2) vector. In **2**, the

Table 6
^{11}B NMR chemical shifts [a] (ppm) in carbaboranes and carbaruthenaboranes

Compound	Chemical shifts [excluding B(3)]	Weighted average
$C_2B_{10}H_{12}$	−1.78(2B) − 8.59(2B) − 12.99(3B) − 14.10(2B)	−9.64
$PhC_2B_{10}H_{11}$	−1.11 −3.40 −7.97(2B) −9.78(2B) −10.29 −11.77(2B)	−8.20
$PhMeC_2B_{10}H_{10}$	−2.36 −3.76 −8.53 (3 or 4B) −9.37 (4 or 3B)	−7.69 or −7.59 [b]
1	2.77 1.25 −6.67(2B) −8.24(2B) −18.59(2B) −23.21	−9.58
3	2.71(2B) −4.27 −6.91 −7.71 −8.15 −14.27 −18.24(2B)	−8.04
4	4.11(2B) −2.05 −4.83 −6.50 −9.30 −11.30 −12.51 −16.07	−6.04

[a] References: $C_2B_{10}H_{12}$ [16]; $PhC_2B_{10}H_{11}$ [21]; $PhMeC_2B_{10}H_{10}$ [6]. [b] It has not proved possible to unambiguously assign the ^{11}B spectrum of $PhMeC_2B_{10}H_{10}$ because of the coincident resonances at −8.53 and −9.37 ppm, in spite of recouse to ^{11}B/^{11}B COSY, ^{1}H-{$^{11}B_{selective}$} and ^{1}H/^{1}H COSY experiments.

value of θ is 68.2(5)°, i.e. 21.8(5)° from eclipsed, with C(16) dipping towards B(6) and C(12) elevated away from B(5). It is of considerable interest to note that in 1-Ph-1,2-*closo*-$C_2B_{10}H_{11}$ the measured θ value is 68.8(6)°, and that ab initio optimization [21] of this parent carbaborane (at the RHF/6-31G* level) affords $\theta = 65.3°$.

The traditional reference plane in icosahedral MC_2B_9 polyhedra [24,25] is the lower boron belt, B(5)B(6)B(11)B(12)B(9). With respect to this, the C(1)–C(11) vector in **2** is inclined at 21.8°, and the arene ring, C(31)–C(36), makes a dihedral angle of 4.7°. Both these values imply a slight degree of interaction between the cage-bound aryl and metal-bound arene groups; arene/B_5 dihedral angles of only 2.3 and 2.1° are observed [4,5] in 3-(C_6H_6)-3,1,2-*closo*-$RuC_2B_9H_{11}$ and 3-(C_6Me_6)-3,1,2-*closo*-$RuC_2B_9H_{11}$, respectively, ascribed to the differing *trans* influences of cage carbon and cage boron atoms [4,26]. Similar crowding between the cage phenyl group and metal-bound η-hydrocarbon has been observed [27] in 1-Ph-3-(C_9H_7)-3,1,2-*closo*-$CoC_2B_9H_{10}$. In the crystallographically determined structure of **2** the nearest arene proton, H(34), lies only 2.89 Å from the plane of the aryl ring, with C(34)–H(34) nearly eclipsing C(1)–C(11). In solution at room temperature, of course, the arene is free to rotate, as illustrated by the ^1H NMR spectrum of **2**.

The two crystallographically independent molecules (**a** and **b**) of compound **4** are of opposite chirality. This notwithstanding, the overall arrangement of {*p*-cymRu} and {$PhMeC_2B_9$} fragments within both molecules are broadly comparable, e.g. the twist of the phenyl group and the relative orientation of the *p*-cym ligand (see later).

Compound **4** was subjected to a crystallographic study to determine whether its cage geometry lay between that of **2** (which is relatively undistorted) and those [20] of 1,2-Ph_2-3-(arene)-3,1,2-*pseudocloso*-$RuC_2B_9H_9$ (which are severely distorted). Unfortunately, the results are somewhat ambiguous. This arises from that fact that although the precision of the structural study of **4** (gauged by, e.g., the typical e.s.d. on a B–B connectivity) is only about half that for the study of **2**, there nevertheless appears to be a measurable difference between the two independent molecules. In molecule **b** C(1)–C(2), 1.702(10) Å, is longer than in **2**, but Ru(3)...B(6), 3.451(9) Å, is not. In fact, the C(1b)–C(2b) distance in **4** is close to that [28] [1.696(5) Å] in the parent carbaborane 1-Ph-2-Me-1,2-*closo*-$C_2B_{10}H_{10}$ although it should be noted that the phenyl orientations (θ) are quite different, 60.1(7) and 16.7(5)°, respectively, and we have already shown [23] that the length of C(1)–C(2) is dependent to some extent on θ. In contrast, molecule **a** displays a fairly long C(1)–C(2) distance, 1.754(11) Å. The possibility that this is merely an artefact of one or both cage carbon atoms being imprecisely located (see caveat to ref. [9]) can probably be rejected in view of the fact fact that Ru(3)...B(6) in **4a** is complementarily short, 3.407(8) Å. Thus it does appear that the molecular structure of **4a** can be interpreted as lying along the 'deformation pathway' from *closo* [exemplified by **2** (and **4b**)] to *pseudocloso* [exemplified by 1,2-Ph_2-3-(C_5Me_5)-3,1,2-*pseudocloso*-$RhC_2B_9H_9$ [2] and 1,2-Ph_2-3-(arene)-3,1,2-*pseudocloso*-$RuC_2B_9H_9$ [20]], albeit much closer to the former. In keeping with this overall conclusion, the {C_2B_9} fragment of molecule **a** fits rather less well against that of our standards 3-(C_6H_6)-3,1,2-*closo*-$RuC_2B_9H_{11}$ and 3-(C_6Me_6)-3,1,2-*closo*-$RuC_2B_9H_{11}$ in rms misfit calculations, 0.051 and 0.048 Å, than does the same fragment of molecule **b**, 0.047 and 0.039 Å, respectively. In each of the calculations involving **4a**, the worst individual atom misfit is for B(6), 0.089 and 0.086 Å, respectively.

The fact that C(1b)–C(2b) is shorter than C(1a)–C(2a) may be consistent with the recognition of rather more crowding between the *p*-cym ligand and the cage-bound phenyl and methyl groups in the **4b**. The *p*-cym ligand is in a rotationally similar position in both molecules (^{i}Pr *trans* to the C_{cage} substituents) with the arene ring/reference B_5 plane dihedral angle 5.6° in **4a** and 7.0° in **4b**. Similarly, the C(1)–C(11) and C(2)–C(21) vectors are relatively depressed in **4b**, making angles of only 19.8 and 18.1°, respectively, to the lower B_5 belt (cf. 21.0 and 18.8°, respectively, in **4a**). Unexpectedly, θ(**4a**) is somewhat greater than θ(**4b**), 60.1(7) (cf. 55.8(7)°).

In sterically distorted *pseudocloso* carbametallaboranes, we have consistently recorded ^{11}B NMR chemical shifts at, on average, very high frequencies relative to those for analogous undistorted species [2,20]. It was therefore of interest to determine whether the beginning of this sort of deformation that is suggested by the structural analysis of **4a** is supported by a similar (albeit smaller) movement to high frequency in the spectrum of **4** (where, of course, "**4a**" and "**4b**" cease to have independent existence). Table 6 lists the weighted average ^{11}B NMR chemical shifts for the 9 relevant boron atoms of various 1,2-dicarbaboranes [no B(3) contribution] and 1,2-dicarba-3-(*p*-cym)ruthenaboranes, measured under identical conditions. As a reference, going from $C_2B_{10}H_{12}$ to $PhC_2B_{10}H_{11}$ to $PhMeC_2B_{10}H_{10}$ causes successive high frequency movements of 1.4 and either 0.5 or 0.6 ppm. In comparison, going from **1** to **3** to **4** results in a similar first movement (1.5 ppm) but a somewhat greater second one (2.0 ppm). The effect is clearly small, but fully

consistent with the overall results of the structural studies: Starting from 3-(*p*-cym)-3,1,2-*closo*-$RuC_2B_9H_{11}$, replacement of one $C_{cage}H$ unit by $C_{cage}Ph$ (**1** → **3**) causes no measureable polyhedral deformation; further replacement of the other $C_{cage}H$ by $C_{cage}Me$ (**3** → **4**) just begins to deform the *closo* polyhedron towards *pseudocloso*. In a forthcoming paper [20], we will report fully on such *pseudocloso* species, formed when the second $C_{cage}H$ is replaced by $C_{cage}Ph$.

Acknowledgements

We thank the University of Edinburgh (JC) and the EPSRC (BDR) for support, the Callery Chemical Company for a generous gift of $B_{10}H_{14}$, and Drs. D. Reed and A.J. Blake for helpful discussions.

References and notes

[1] Part 6: T.D. McGrath and A.J. Welch, *Acta Crystallogr., Sect. C, 50* (1994) in press.

[2] Z.G. Lewis and A.J. Welch, *J. Organomet. Chem., 430* (1992) C45. Note that the signs of two of the ^{11}B NMR chemical shifts of compound II reported in Table 1 of this paper are in error, and should read +10.3(2B) and +4.0(2B).

[3] D.R. Baghurst, R.C.B. Copley, H. Fleischer, D.M.P. Mingos, G.O. Kyd, L.J. Yellowlees, A.J. Welch, T.R. Spalding and D. O'Connell, *J. Organomet. Chem., 447* (1993) C14.

[4] M.P. Garcia, M. Green, F.G.A. Stone, R.G. Somerville, A.J. Welch, C.E. Briant, D.N. Cox and D.M.P. Mingos, *J. Chem. Soc., Dalton Trans.*, (1985) 2343.

[5] X.L.R. Fontaine, N.N. Greenwood, J.D. Kennedy, J. Plesek, B. Stibr and M. Thornton-Pett, *Acta Crystallogr., Sect. C, 46* (1990) 995.

[6] T.D. McGrath and A.J. Welch, unpublished results.

[7] M.A. Bennett and A.K. Smith, *J. Chem. Soc., Dalton Trans.*, (1974) 233.

[8] M.A. Bennett, T.-N. Huang, T.W. Matheson and A.K. Smith, *Inorg. Synth., 21* (1982) 74; α-terpinene used in place of α-phellandrene.

[9] P.T. Beurskens, W.P. Bosman, H.M. Doesbury, T.E.M. van den Hark, P.A.J. Prick, J.H. Noordik, G. Beurskens, R.O. Gould and V. Parthasarathai, *DIRDIF; Applications of Direct Methods to Difference Structure Factors*, University of Nijmegen, The Netherlands, 1983. It is possible that the crystallographic pseudosymmetry in **4** could result in imprecise atomic co-ordinates.

[10] N.G. Walker and D. Stuart, *Acta Crystallogr., Sect. A, 39* (1983) 158.

[11] G.M. Sheldrick, *SHELX-76; Program for Crystal Structure Refinement*, University of Cambridge, 1976.

[12] *International Tables for X-Ray Crystallography*, Vol. 4, Kynoch Press, Birmingham, 1974, p. 99.

[13] R.O. Gould and D.E. Smith, *CADABS; Program for Data Reduction*, University of Edinburgh, 1986.

[14] R.O. Gould and P. Taylor, *CALC; Program for Molecular Geometry Calculations*, University of Edinburgh, 1986.

[15] G.M. Sheldrick, *SHELXTL (PC version 4.2)*, University of Gottingen, Germany, 1990.

[16] K.F. Shaw and A.J. Welch, *Polyhedron, 11* (1992) 157.

[17] T.P. Hanusa, J.C. Huffman and L.J. Todd, *Polyhedron, 1* (1982) 77.

[18] K.F. Shaw, B.D. Reid and A.J. Welch, *J. Organomet. Chem.*, in press.

[19] M. Bown, J. Plesek, K. Base, B. Stibr, X.L.R. Fontaine, N.N. Greenwood and J.D. Kennedy, *Magn. Reson. Chem., 27* (1989) 947.

[20] P.T. Brain, M. Bühl, J. Cowie, Z.G. Lewis and A.J. Welch, in preparation.

[21] P.T. Brain, D.J. Donohoe, D. Hnyk, M. Bühl, D.W.H. Rankin, H.E. Robertson, D. Reed and A.J. Welch, in preparation.

[22] S.A. Macgregor, A.J. Wynd, N. Moulden, R.O. Gould, P. Taylor, L.J. Yellowlees and A.J. Welch, *J. Chem. Soc., Dalton Trans.*, (1991) 3317.

[23] Z.G. Lewis and A.J. Welch, *Acta Crystallogr., Sect. C, 49* (1993) 705. The present definition of θ slightly modifies that previously used.

[24] D.M.P. Mingos, M.I. Forsyth and A.J. Welch, *J. Chem. Soc., Dalton Trans.*, (1978) 1363.

[25] D.E. Smith and A.J. Welch, *Acta Crystallogr., Sect. C, 42* (1986) 1717.

[26] G.K. Barker, M.P. Garcia, M. Green, G.N. Pain, F.G.A. Stone, S.K.R. Jones and A.J. Welch, *J. Chem. Soc., Chem. Commun.*, (1981) 652 and refs. therein.

[27] Z.G. Lewis, D. Reed and A.J. Welch, *J. Chem. Soc., Dalton Trans.*, (1992) 731.

[28] T.D. McGrath and A.J. Welch, *Acta Crystallogr., Sect. C, 50* (1994) in press.